BMC Cell Biology

Research article

Effects of "second-hand" smoke on structure and function of fibroblasts, cells that are critical for tissue repair and remodeling

Lina S Wong[1,2], Harry Miguel Green[1], Jo Ellen Feugate[1], Madhav Yadav[3], Eugene A Nothnagel[3] and Manuela Martins-Green*[1]

Address: [1]Department of Cell Biology and Neuroscience, University of California, Riverside, California, USA, [2]Division of Biomedical Sciences, University of California, Riverside, California, USA and [3]Department of Botany and Plant Sciences, University of California, Riverside, California, USA

Email: Lina S Wong - lwong@citrus.ucr.edu; Harry Miguel Green - harryg@caltech.edu; Jo Ellen Feugate - feugate@earthlink.net; Madhav Yadav - madhav.yadav@ucr.edu; Eugene A Nothnagel - nothnagl@citrus.ucr.edu; Manuela Martins-Green* - mmgreen@mail.ucr.edu

* Corresponding author

Published: 05 April 2004

BMC Cell Biology 2004, **5**:13

Received: 07 November 2003

Accepted: 05 April 2004

This article is available from: http://www.biomedcentral.com/1471-2121/5/13

Abstract

Background: It is known that "second-hand" cigarette smoke leads to abnormal tissue repair and remodelling but the cellular mechanisms involved in these adverse effects are not well understood. Fibroblasts play a major role in repair and remodelling. They orchestrate these processes by proliferating, migrating, and secreting proteins such as, cytokines, growth factors and extracellular matrix molecules. Therefore, we focus our studies on the effects of "second-hand" cigarette smoke on the structure and function of these cells.

Results: We used sidestream whole (SSW) smoke, a major component of "second-hand" smoke, primary embryonic fibroblasts, cells that behave very much like wound fibroblasts, and a variety of cellular and molecular approaches. We show that doses of smoke similar to those found in tissues cause cytoskeletal changes in the fibroblasts that may lead to a decrease in cell migration. In addition, we also show that these levels of cigarette smoke stimulate an increase in cell survival that is reflected in an increase and/or activation of stress/survival proteins such as cIL-8, grp78, PKB/Akt, p53, and p21. We further show that SSW affects the endomembrane system and that this effect is also accomplished by nicotine alone.

Conclusions: Taken together, our results suggest that: (i) SSW may delay wound repair because of the inability of the fibroblasts to migrate into the wounded area, leading to an accumulation of these cells at the edge of the wound, thus preventing the formation of the healing tissue; (ii) the increase in cell survival coupled to the decrease in cell migration can lead to a build-up of connective tissue, thereby causing fibrosis and excess scarring.

Background

Although it was believed for a long time that cigarette smoke only affects those who smoke, since the early 1980s we have known that non-smoking wives and children of smokers have twice the risk of dying from lung cancer as those of wives and children in non-smoking households [1]. Consequently, adults and children living in the homes of smokers and workers in environments that contain "second-hand" cigarette smoke can be almost

as adversely affected by the toxic substances of tobacco smoke as the smokers themselves.

Cigarette smoke is a complex mixture of many toxic substances. There are primarily two types of smoke: first-hand smoke (inhaled by the smoker) and second-hand smoke (inhaled by non-smokers in places where smoking is allowed). Second-hand smoke is composed primarily of smoke that emanates from the end of the burning cigarette, smoke that the smoker exhales, and contaminants that diffuse through the cigarette paper [2]. These two types of smoke have basically the same composition except that in second-hand smoke many components are more concentrated than in first-hand smoke [2,3]. For example, nicotine, tar, nitric oxide, and carbon monoxide levels are at least two times more abundant in second-hand smoke, and aromatic amines, such as the carcinogens o-toluidine, 2-naphthylamine, and 4-aminobiphenyl, are preferentially formed in second-hand smoke [2,3]. Therefore, it is possible that the increased risk for people's health when exposed to second-hand smoke lies in the fact that the toxic substances are highly concentrated in this type of smoke [2].

Cigarette smoking causes numerous adverse effects, some of which are associated with poor healing [4,5]. However, the specific cellular effects of this type of stress on repair and remodeling are still poorly understood. Only within the last few years has it been shown in laboratory models that passive smoking decreases blood flow to the wound site [6] and intermittent smoke inhalation delays granulation tissue development and remodeling [7]. Therefore, non-smokers who have undergone surgery, and diabetic children and adults who heal poorly, may suffer significantly from the presence of second-hand cigarette smoke.

Fibroblasts are critical for many aspects of repair and remodeling. For example, shortly after initiation of the healing process, fibroblasts synthesize, deposit, and remodel the extracellular matrix (ECM), a process that is critical for both the migration of endothelial cells to form blood vessels, and the migration of a new wave of fibroblasts to promote healing. Once the fibroblasts have migrated into the wound site, they become profibrotic and produce collagen-type ECM, acquire a contractile phenotype, and contract to close the wound. The development of this fibroblast-rich healing tissue is tightly regulated, and any deregulation of the aforementioned processes will result in impaired healing, leading to open wounds, or in excess healing, causing fibrosis and excess scarring [8]. Any cellular stress that affects the structure or function of these cells may affect the repair and remodeling processes.

The studies presented here were designed to determine the effects of soluble components in second-hand cigarette smoke on fibroblast structure and function. For this purpose, we generated Side-Stream Whole (SSW) smoke solutions, a complex mixture of many of the components of "second-hand" smoke [2,3], and performed our studies using chicken embryonic fibroblasts because it has been known for several years that embryonic fibroblasts behave similarly to wound fibroblasts [9]. We show that doses of SSW smoke that are similar to those found *in vivo* affect the endomembrane system, and that nicotine can mimic this effect. Furthermore, SSW causes a decrease in fibroblast migration and stimulates cellular stress responses that contribute to cell survival. These effects can contribute to abnormal healing and may explain why people who are consistently exposed to "second-hand" smoke suffer from slow healing and excessive scarring of wounds, much like smokers themselves.

Results

To ensure that the same amounts of SSW smoke components were added to the cells in each study and to ensure that we were exposing the cells to doses of smoke similar to those found in tissues *in vivo*, the smoke solutions used were always prepared in the same way and were quantified based on the levels of nicotine. Nicotine was used as a biomarker to measure the amount of smoke components added to the cells because it is one of the most abundant and stable components in tobacco smoke, is commonly used as a biomarker in tobacco studies [2,10,11], and can easily be measured by gas chromatography in our smoke solutions. The amount of nicotine in the SSW solutions was ~20 μg/ml/cigarette. In urban non-smokers the average concentration of nicotine in the urine was 0.010 μg/ml with a range of 0–0.064 μg/ml, but after spending 78 minutes in a smoky room this average increased to 0.080 μg/ml (range 0.013–0.208 μg/ml) [12]. The amount of nicotine accumulated in tissues can be 15 to 25 times higher [13,14]. Therefore, for the studies presented here, we used levels of SSW approximating concentration ranges of nicotine in the tissues of passive smokers (1:9 dilution, smoke solution:media, contains ~2.0 μg/ml of nicotine). To perform our studies we used embryonic fibroblasts because it has been shown that these cells resemble wound fibroblasts [9].

Effects of SSW on fibroblast structure

Exposure of chicken embryonic fibroblasts to SSW smoke solutions resulted in a change in appearance of the cultures, from the cells being flattened and contact inhibited in the control to becoming more elongated and well separated from each other in the smoke treated cells (Fig. 1A,1B). These effects were observed with smoke concentrations similar to those found in tissues (1:9; SSW:media), whereas at higher doses (1:4), the cells

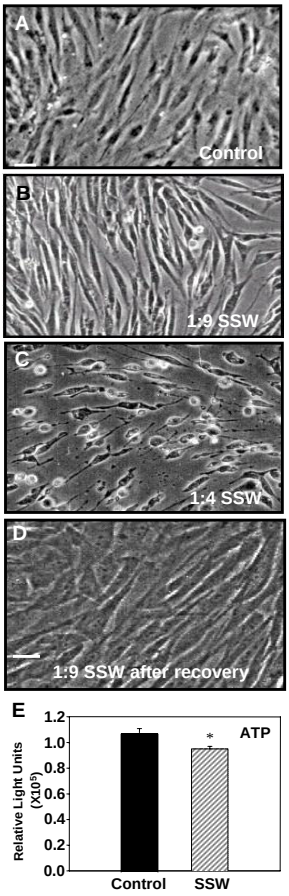

Figure 1
Phase-contrast microscopy analysis of sidestream whole (SSW) smoke treated primary fibroblasts. Cells were treated with different doses of SSW for 18 hours. Control cells were kept in serum-free medium for the same time period because the smoke solutions are diluted in serum-free medium. **(A)** Untreated cells were spread out, confluent, contact inhibited, and showed prominent nuclei. **(B)** Cells treated with 1:9 (SSW:media) smoke dilution became elongated and separated from each other. **(C)** Cells treated with 1:4 SSW smoke rounded up and showed signs of cell death. **(D)** Cells treated with 1:9 SSW smoke solution recovered quickly; within a few hours of being in complete media they were back to normal morphology. **(E)** ATP assays: cells were plated in a 96 well ELISA plate, allowed to reach confluency, and treated for 18 hours with SSW. Smoke-treated cells showed a decrease in ATP production, but the overall ATP level remained high. Pictures are representative of at least 3 experiments performed with different batches of primary cells. Scale bar = 20 μm.

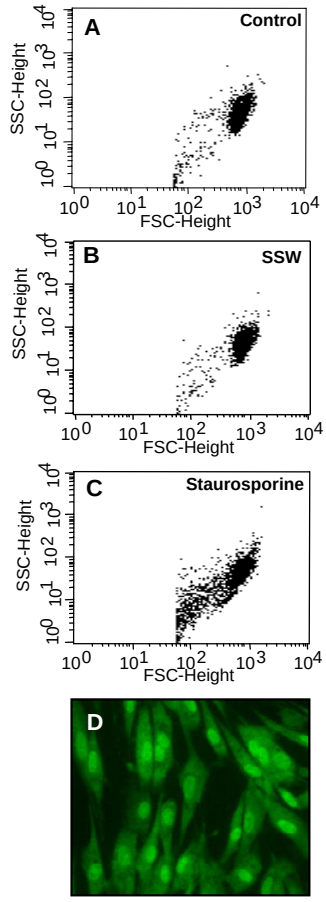

Figure 2
Flow cytometric analysis of cells treated with SSW smoke. Cells were treated with 1:9 SSW smoke or with staurosporine and analyzed by flow cytometry to determine the forward- and side-scattering properties of the cells. **(A&B)** Untreated and SSW-treated cells show similar pattern of forward- and side-scattering properties. **(C)** Staurosporine treated cells (positive control) showed more cells with lower forward-scattering properties than either control or SSW-treated cells suggesting that SSW smoke is not causing cell death and that the overall structure of the cell is normal. The graphs represent 10,000 events. **(D)** Acridine-orange and ethidium bromide staining; cells showed normal morphology, and no blebbing of the nucleus or plasma membrane was observed. *SSC = side-scatter, FSC = forward-scatter*. Figures are representative of at least 3 repeated studies. Scale bar = 20 μm.

rounded up, underwent cell death and floated into the culture medium (Fig. 1C). In order to confirm that the 1:9 concentration of SSW smoke components does not cause cell death, we performed several assays. We removed the smoke-containing medium and added fresh medium to the cultures to see if the cells recovered from the smoke exposure; within a few hours, the cells flattened and contacted each other again, and by 18 hours, the cultures

returned to a normal state (Fig. 1D). We also performed a cell viability test by measuring the concentration of cellular ATP in cells treated with concentrations of 1:9 (SSW:media). Although SSW-treated cells produced less ATP than the control cells, the levels remained high (Fig. 1E), indicating that the doses of smoke we use in our studies do not result in severe metabolic alterations. Further, we performed flow cytometric analysis and found that untreated and SSW-treated cells showed high forward scattering properties (Fig. 2A,2B) with very few cells having low forward scattering properties, indicating a healthy morphology. On the other hand, staurosporine treatment (positive control), resulted in the majority of the cells showing much lower forward scattering properties (Fig. 2C), an indication that the cells were more fragmented or had a rough surface which is usually indicative of membrane blebbing and cell death. These findings were confirmed by staining the cells with acridine-orange/ethidium bromide to ascertain that the nucleus and the plasma membrane did not show blebbing (Fig. 2D). Taken together these data show that doses of SSW smoke approximating those found in tissues *in vivo* do not cause death of fibroblasts. Therefore, we tested a number of processes that can potentially be affected by these doses of SSW smoke, and might contribute to the abnormal healing observed in people that are exposed to this type of smoke.

Effects of SSW on cell survival

To test whether cell proliferation was affected by SSW smoke solutions, fibroblasts were treated as above and cultured in the presence or absence of BrdU (Bromo-deoxyUridine). At the end of the experiment, the cells cultured in the absence of BrdU were counted using a Coulter counter. We observed that the smoke treatment did not significantly affect cell number (Fig. 3A). Cultures treated with BrdU were assayed for BrdU incorporation and showed that SSW inhibits cell division (Fig. 3B). This apparently conflicting result led us to hypothesize that these concentrations of SSW stimulate fibroblasts to survive by stimulating these cells to express and/or activate stress-response and/or survival proteins. To test this possibility, we examined the expression and activation of proteins that are known to be involved in cell survival or stress responses, such as the early stress response protein, interleukin-8 (cIL-8), the survival protein, protein kinase B (PKB/Akt), the ER stress response protein, glucose-regulated protein 78 (grp78), and the cell cycle control and survival proteins, p53 and p21. Cells responded to the smoke exposure by stimulating cIL-8 in a dose dependent manner (Fig. 4A); PKB/Akt was rapidly activated, peaking 5 minutes after initiation of smoke treatment (Fig. 4B); grp78 (Fig. 4C), p53 (Fig. 4D), and p21 (Fig. 4E) were also stimulated, albeit to different levels. These results coupled with those described in figure 3 suggest that the cells exposed to these doses of SSW smoke may be surviving better than the untreated cells. To test this possibility, we treated the cultures with SSW smoke for 18 hours, followed by replacement of the treatment with fresh medium for 24 hours, a time period that is sufficient to allow these cells to undergo at least one round of cell division. During this time, the cells recovered well from the stress caused by cigarette smoke and acquired a healthy morphology much like those of the control. The cells were then treated again with SSW for 18 hours to determine whether they would survive well after multiple rounds of SSW treatment. At the end of the experiments the cells were counted; the number of cells in the control and SSW-treated cultures were virtually the same (Fig 4F). Because the cells exposed to SSW replicate poorly (see Fig. 3B), the results taken together suggest that SSW increases cell survival.

Effects of SSW on cell migration

Figure 1B shows that SSW-treatment induces a change in cell shape, leading us to examine whether alterations occur in major cytoskeletal elements involved in cell shape changes such as microfilaments. To perform these studies, we used rhodamine phalloidin to label F-actin. SSW-treatment increased stress fiber formation, as observed both by fluorescent labeling (Fig. 5A,5B) and by quantification of F-actin (Fig. 5C). Because stress fibers are known to associate with proteins in focal adhesion plaques to anchor cells to the substratum, we treated the cells with SSW, then visualized focal adhesion plaques by immunolabeling for vinculin. Smoke treatment increased focal adhesion plaque formation (Fig. 5D,5B). Furthermore, immunoblot analysis to quantify the levels of vinculin in treated cells showed that this protein is increased (Fig. 5F). GAPDH was used to control for loading (see Fig. 4C). These findings raise the possibility that SSW affects cell motility by increasing cell adhesion to the substratum. We used the cloning ring migration assay to test the possibility that cell migration is affected. In this assay, cells were seeded inside a cloning ring and allowed to adhere to the plate to form a "circle of cells" with a defined edge. After application of the treatment for the indicated time point, the distance migrated by the cells was measured from the edge of the original "circle of cells" to the fibroblasts that were furthest from the edge. SSW-treated cells (Fig. 5H,5I) were unable to migrate to the same extent as the control cells (Fig. 5G). Taken together, these data suggest that doses of SSW smoke comparable to those found in tissues *in vivo* adversely affect the cytoskeleton of fibroblasts, resulting in functional alterations, such as increased cell adhesion, leading to a decrease in cell migration.

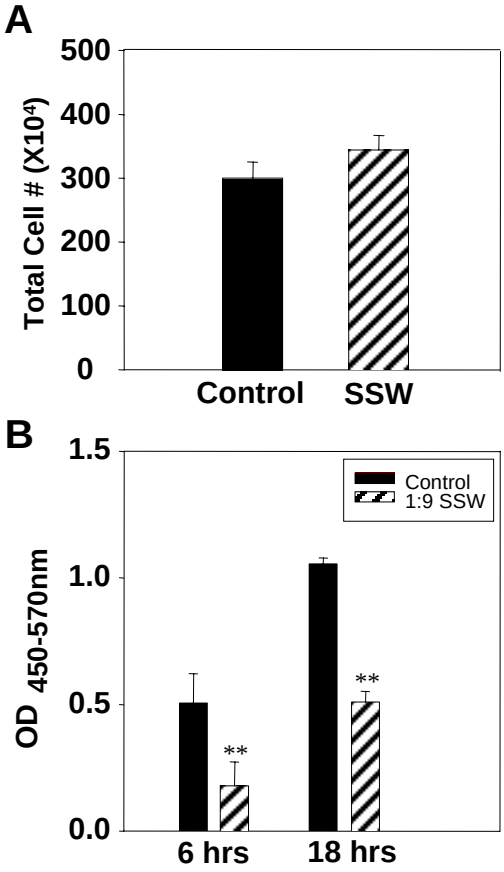

Figure 3

Effects of SSW smoke on fibroblast growth. **(A)** Cells were treated for 18 hours with SSW smoke solution and the total cell number was counted using a Coulter counter with a specified particle size of 7 μm to 20 μm. There was no significant difference between controls and treated cells. **(B)** Primary fibroblasts were plated in 96-well plates and allowed to grow to confluency and BrdU alone or BrdU plus SSW were added to the cultures and the cells were allowed to incorporate the BrdU for the indicated time points. At both 6 and 18 hours, SSW-treated cells showed a significant decrease in BrdU incorporation when compared to the control. Experiments are performed at least two times with different batches of primary fibroblasts. *OD = Optical Density*.

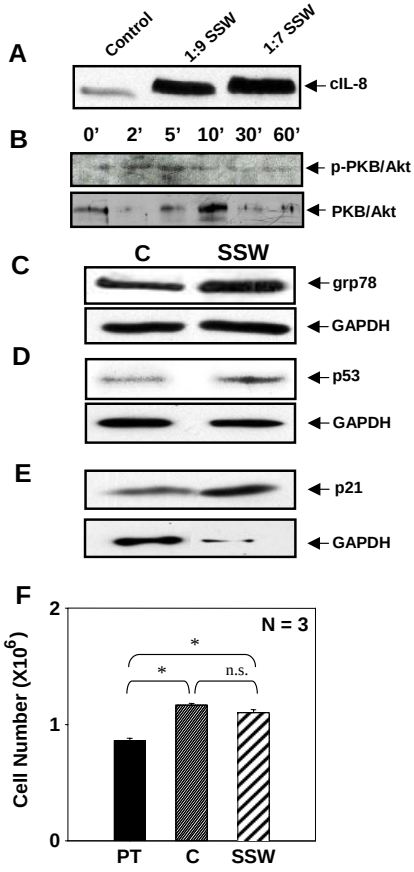

Figure 4

SSW smoke stimulates stress response proteins and cell survival. SSW stimulated an increase in immediate early stress-response proteins as assayed by immunoblotting analysis. **(A)** cIL-8 was stimulated in a dose-dependent manner. **(B)** PKB/Akt was phosphorylated/activated by 5 minutes. **(C-E)** The levels of grp78 **(C)**, p53 **(D)**, and p21 **(E)** were all increased upon stimulation with SSW smoke. GAPDH was used as a marker for levels of sample loading. Because the supernatant does not contain GAPDH, we verified equal loading for cIL-8 by using coomassie blue staining of identical samples. **(F)** Cells were treated for 18 hours, allowed to recover in fresh medium for 24 hours, treated again for 18 hours and then counted using a Coulter counter. The number of cells after SSW treatment was comparable to that of the control, suggesting that cells survived well even though they were cultured in the presence of SSW smoke. For immunoblotting analysis, cells were treated and lysates separated using SDS-PAGE. Each figure is a representative of at least 2 experiments. PT = Pretreatment; N = 3 indicates 3 samples per experimental group.

Effects of SSW on the endomembrane system

In addition to the findings described above, we also observed that SSW treatment causes the appearance of numerous vacuoles in the cytosol within 3–4 hours after treatment was initiated (Fig. 6A). To determine the origin of vacuolation, we prepared the cells for analysis by transmission electron microscopy. Early times after exposure to SSW were used because at these time points the organelles are still clearly identified. Four hours after treatment with SSW, we observed that the cells were still

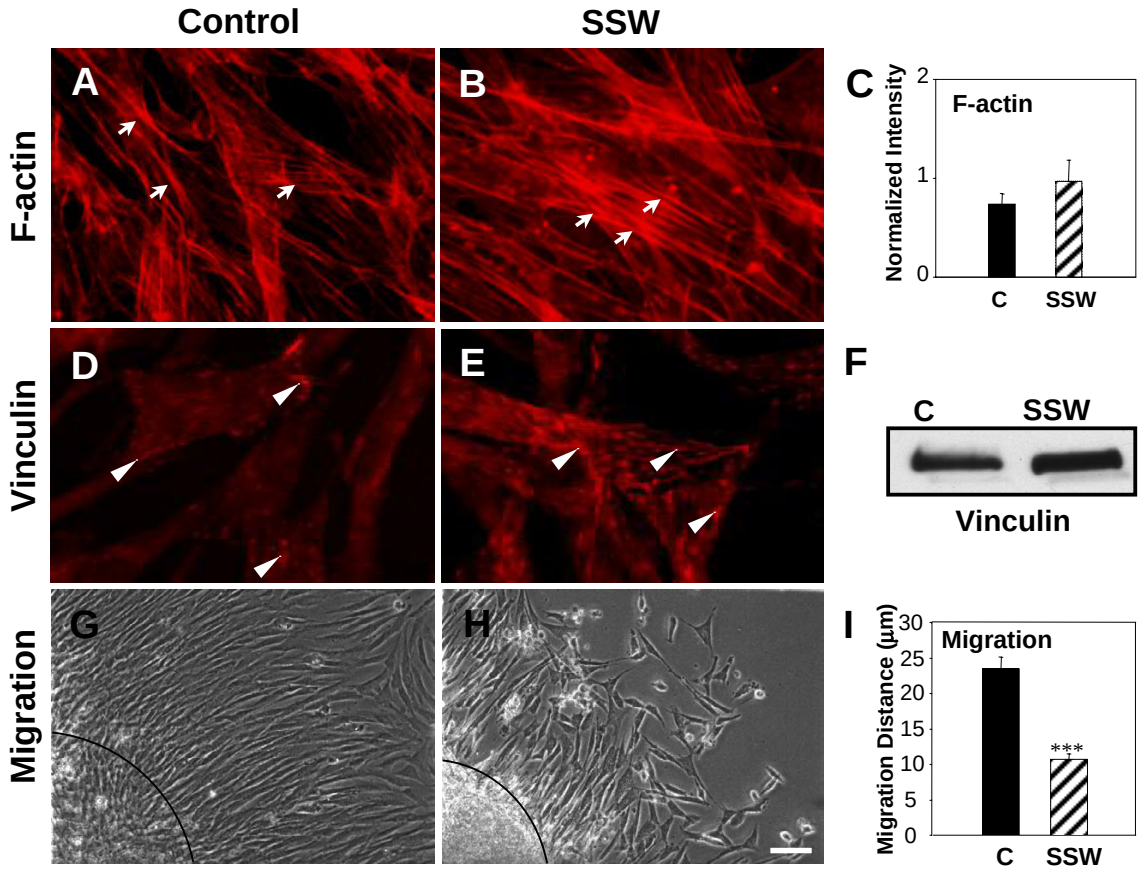

Figure 5

Effects of SSW smoke on microfilaments and focal adhesion plaques. Cells were treated with 1:9 smoke dilutions and different markers were analyzed. **(A, B)** Rhodamine-phalloidin labeling of F-actin showed that treated fibroblasts have more F-actin staining and the stress fibers appeared thicker. **(C)** The increase in F-actin was confirmed by staining the cells and measuring the amount of rhodamine-phalloidin present in the cells using a fluorimeter at 550–580 nm. **(D, E)** Fluorescence images of cells treated with SSW smoke and labeled for the focal adhesion plaque protein, vinculin. Smoke treated cells showed an increased in focal adhesion plaque formation compare with control cells. **(F)** Immunoblot analysis for vinculin confirms that SSW stimulates an increase in vinculin levels. For equal loading of protein in the immunoblots, please refer to grp78 blots in Fig. 4C; the same membrane was used to reprobe for the protein shown in this figure. **(G, H)** Effects of SSW on cell migration. Cells were plated inside cloning rings and allowed to adhere for 3 hours to form a "ring of cells". After marking the edge of the ring, the cells were treated and allowed to migrate for 24 hours and the migrated distance was measured from the edge of the ring to the migrating front of the cells. The treated cells showed a decrease in cell migration. **(I)** Quantification of the extent of inhibition of cell migration by SSW smoke. Data are representative of six different points along the circle. Dashed lines in G&H demark the edge of the "circle of cells". All experiments were performed at least 3 times with different batches of primary cells. Scale bar = 20 μm.

morphologically unaffected (Fig. 6B); the mitochondria (Fig. 6C) and the nucleus (Fig. 6D) were morphologically normal whereas the endomembrane system was dilated and irregularly shaped (Fig. 6E). For comparison the endomembrane system of untreated cells is also shown (Fig. 6F). We further analyzed the integrity of the endomembrane system by staining with $DIOC_6$, a dye commonly used to label the endoplasmic reticulum (ER). The control cells showed that the ER was well developed, concentrated around the nucleus but also spread throughout the cytosol (Fig. 7A), whereas SSW-treated cells showed punctated staining, indicating fragmentation and

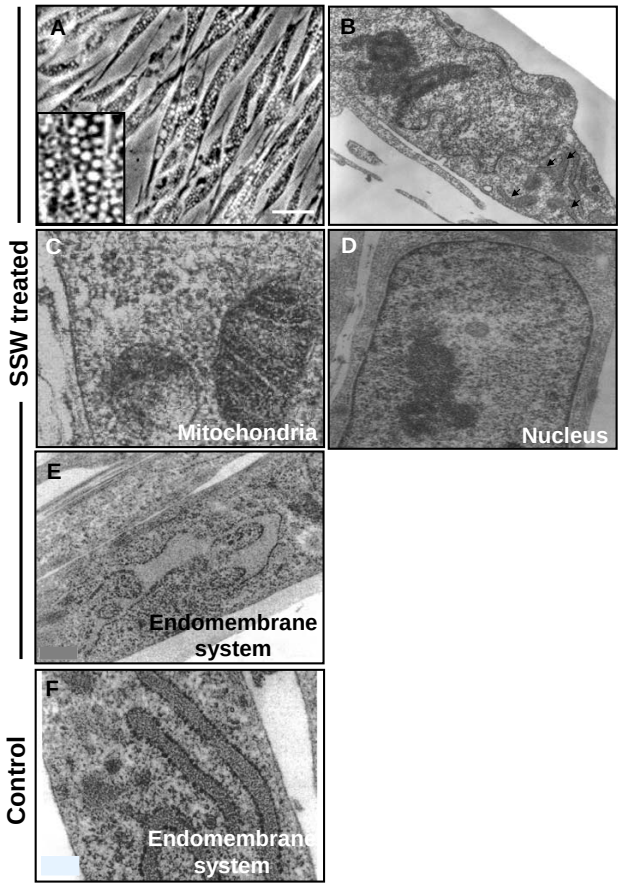

Figure 6
Microscopic analysis of cells treated with SSW smoke. **(A)** SSW-treated cells developed numerous vacuoles in the cytosol. Inset shows a higher magnification of the vacuoles. **(B-F)** Cells treated with SSW for 4 hours were fixed and prepared for Transmission Electron Microscopy (TEM). We observed that the cells are still morphologically intact **(B)** except for the endomembrane system, which is beginning to show swelling (arrows). However, most organelles, such as the mitochondria **(C)** and the nucleus **(D)** look normal, whereas the endomembrane system is irregularly shaped and shows signs of swelling **(E)**. **(F)** Endomembrane system of untreated cells. Scale bars = 20 μm in (A), 5 μm in (B) and 0.6 μm in (C-F).

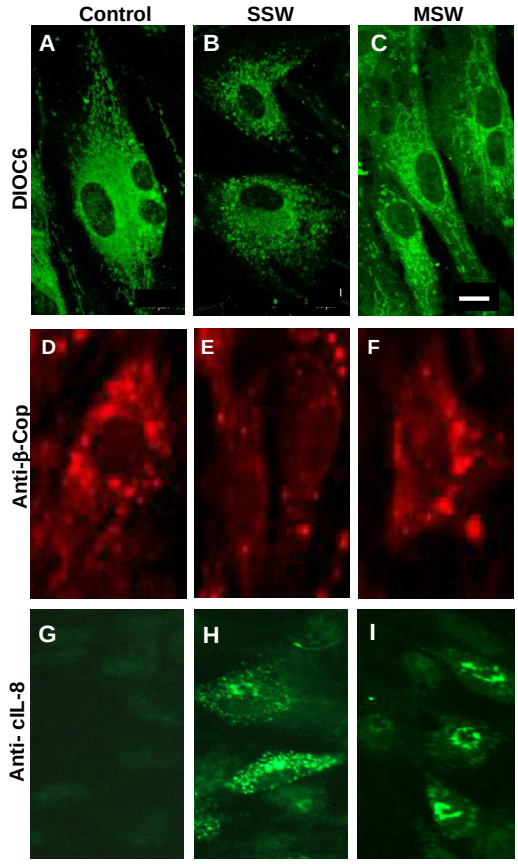

Figure 7
SSW smoke affects the endomembrane network. Cells were exposed to 4 or 8 hours of smoke treatment (SSW or MSW) and prepared for fluorescence imaging. **(A)** Confocal microscopy analysis of DIOC6 stained cells. Untreated cells show normal ER network concentrated around the nucleus and also spread out to the periphery of the cell. **(B)** SSW treated cells show that the ER is fragmented when compared with the control and is only found around the nucleus. **(C)** MSW-treated cells show similar ER morphology to that of the control. **(D-F)** To ascertain the status of the Golgi network, we used anti-β-COP monoclonal antibody for immunocytochemistry, which specifically labels the Golgi network. **(D)** In untreated cells, the staining of the Golgi surrounds the nucleus and vesicles are seen all over the cytosol. **(E)** In SSW-treated cultures, the cells have many fewer Golgi vesicle staining. **(F)** MSW treated cells show an organization similar to that found in the control. **(G-I)** Fibroblasts were treated as above and immunolabeled for cIL-8. **(G)** In untreated cells, the expression of cIL-8 is barely present because this protein is only expressed when it is stress-induced. **(H)** SSW-treated cells were observed to have no perinuclear staining; instead, the endomembrane system was dispersed throughout the cytosol. **(I)** MSW-treated cells show that the cIL-8 is being produced in the endomembrane system near the nucleus where this normally occurs. Pictures are representative of 2 different experiments. Scale bars = 50 μm in (A-F) and 30 μm in (G-I).

coalescence of this membranous system around the nucleus (Fig. 7B). This effect is specific for SSW; cells treated with MainStream-Whole smoke (MSW), a solution that mimics "first-hand" smoke [10], did not affect the ER and looked very much like the control (Fig. 7C). To further examine the SSW-induced alteration in the endomembrane system, we stained the cells with an antibody to β-COP, a protein present in the Golgi network

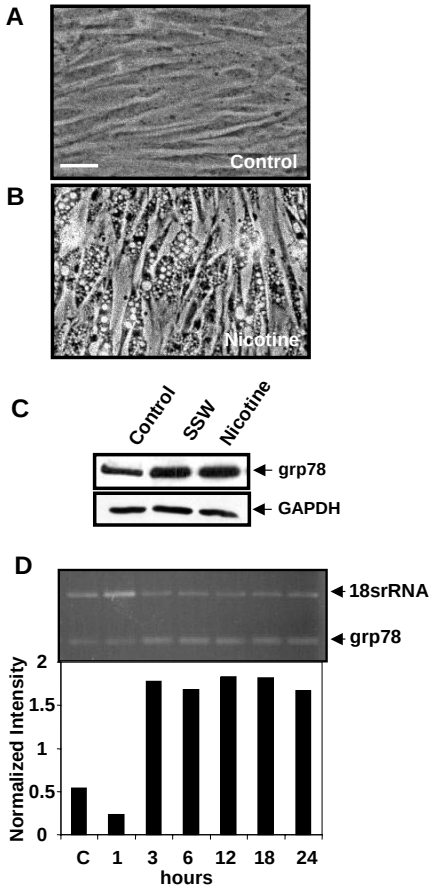

Figure 8
Nicotine mimics the effects of SSW smoke on the endomembrane. **(A&B)** Phase contrast microscopy of cells treated with 1.5 mM nicotine for 4 hours showed vacuolation similar to that found in fibroblasts treated with SSW smoke (Compare with Fig. 6A). **(C)** Western blot analysis showing that nicotine stimulated grp78 expression, an ER specific stress response protein, to similar levels as SSW. GAPDH shows equal loading of cell lysate. **(D)** RT-PCR of nicotine-treated cells showed that this component of smoke stimulated grp78 expression. Data are representative of at least 3 different studies with 3 different batches of primary cells. Scale bar = 20 μm.

and vesicles. Again, in the control and MSW treated cells, the staining showed well-distributed Golgi vesicles in the Golgi network, whereas after SSW treatment, the staining was much less abundant suggesting breakdown of the network (Fig. 7D,7E,7F). In addition, we investigated the specific effects of SSW treatment on the endomembrane system, by examining the pattern of secretion of the chemokine, cIL-8, a protein that goes through the ER and Golgi before leaving the cell. Because cIL-8 is an inducible chemokine and is stimulated by stress-inducing agents, it is not produced under normal conditions (Fig. 7G). However, SSW-treated fibroblasts showed virtually no perinuclear staining where it would be expected; rather cIL-8 was dispersed throughout the cytoplasm suggesting a disruption of the endomembrane system (Fig. 7H). MSW-treated cells, on the other hand, showed perinuclear staining indicating that the cells have been stimulated by the smoke to produce cIL-8 and synthesis of the protein is occurring in close association with the nuclear membrane (Fig. 7I).

Second-hand smoke is very rich in nicotine, 2–3 times higher than in MSW (first-hand) smoke [2], and nicotine has been reported to cause vacuolation in cells. We found that nicotine is able to cause the vacuolation in fibroblasts to the same extent as SSW (compare Figs. 6A and 8B), suggesting that nicotine is at least a partially responsible for the effects of SSW on the endomembrane system. As mentioned above, grp78 is an intracellular molecule that is stimulated/activated when cells are under stress [15-18] and has also been shown to be specifically stimulated by agents that induce ER stress [19-21]. We found that nicotine stimulates grp78 to levels similar to those stimulated by SSW, both for the protein (Fig. 8C) and the mRNA (Fig. 8D). This suggests that nicotine is a major player in the effects of SSW on the changes we observe in the endomembrane system.

It is well established that the endomembrane system is intricately connected to microtubules for its distribution and function. We investigated the possibility that the microtubule network was altered in the smoke treated cells. In the control cells, the microtubules emanate from the perinuclear region, where the centrosome or microtubule organizing center (MTOC) is located, with clear, organized extension of the microtubules throughout the cytoplasm in all directions (Fig. 9A). In SSW-treated cells, the MTOC was disorganized and much less localized than in the control cells, and the microtubules did not project out from the MTOC into the cytosol in an organized manner, suggesting disruption of the tubulin arrays (Fig. 9B). To determine whether the levels of tubulin in the cells treated with SSW were altered, we performed immunoblot analysis and found that the SSW treated cells contained a higher level of tubulin than those of the untreated cells (Fig. 9C). Equal loading was confirmed using GAPDH as an internal control (see Fig. 4C; the same membrane was used to reprobe for the protein shown in this figure).

Effects of SSW on wound healing

During granulation tissue formation, it is necessary for fibroblasts to migrate to the wound area in order to perform their many functions. Indeed, if migration is

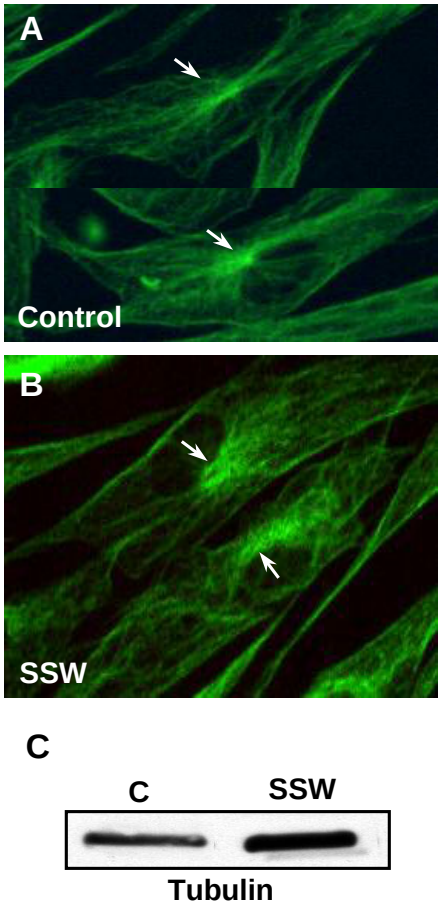

Figure 9
The effects of SSW on microtubules. **(A, B)** Fluorescence images of microtubules labeled with an antibody to tubulin. **(A)** Control cells showed a characteristic, brightly labeled microtubule organizing center (MTOC=centrosome) with microtubules radiating outward throughout the cytoplasm. **(B)** SSW-treated cells showed a much less orderly extension of the tubules, and the MTOC were much less organized than in the control cells. **(C)** Immunoblot analysis showed an increase in tubulin after smoke treatment. For equal loading of protein in the immunoblots, please refer to grp78 blots in Fig. 4C; the same membrane was used to reprobe for the protein shown in this figure.

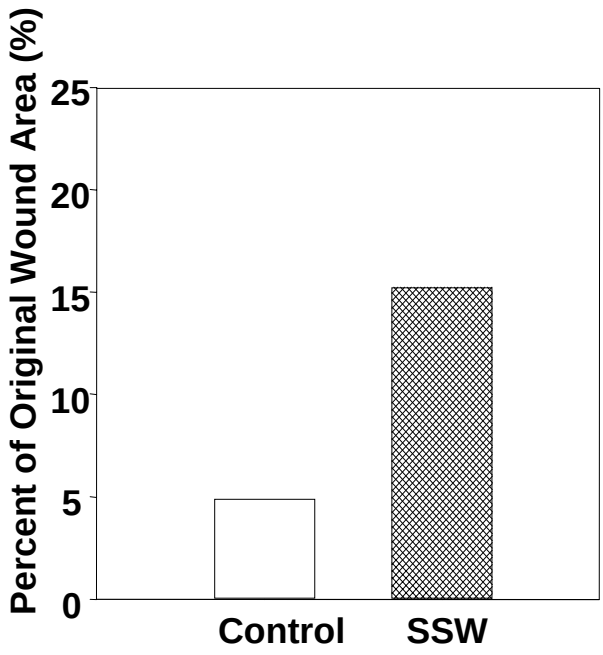

Figure 10
Effect of SSW smoke on wound closure. Mice were wounded with a 5 μm biopsy punch, pictures were taken at 5 and 7 days with 7.5× magnification. The areas of the wounds were quantified using Scion Image Software. By 7 days, the wounds of the control animals were approximately 95% closed whereas SSW wounds were only 85% closed. Data show the results of two representative experiments.

inhibited, as shown above, granulation tissue formation would be defective, resulting in slow or partial wound closure. In order to test this possibility, we performed wound healing assays in mice (C57BL/6J) that had been smoking for six months. The wounds were made with a 5 mm biopsy punch to the back of the mice and pictures were taken at the same magnification at day zero and day seven. The areas of the wounds were measured using Scion Image (NIH Image) and percent of the original wound area was calculated. At seven days, the area of the wounds of mice not exposed to smoke was 95% closed whereas the wounds of the SSW-exposed mice were only 85% closed (Fig. 10), showing that wound closure is significantly delayed by smoking. Cross-sections through the wounds of these mice showed that the granulation tissue of the smoking mice have abnormal cellularity and matrix deposition.

Discussion

It is well known that cigarette smoking is very damaging to the body, resulting primarily in cell death and in mutations of DNA that can lead to cancer [22-36]. Less well known are the effects of doses of cigarette smoke that do

not cause cell death in tissues of second-hand smokers. Here we show that SSW cigarette smoke, a major component of second-hand smoke, affects fibroblasts at various levels: (i) It stimulates changes in the endomembrane system, including activation of the ER stress response protein grp78; these effects are reversible, can also be induced by nicotine alone and may be dependent on microtubule integrity. (ii) It enhances production/activation of several other stress/survival response proteins. (iii) It may increase cell survival. (iv) It alters the cytoskeleton and stimulates focal adhesion plaque formation resulting in inhibition of cell migration. (v) It inhibits wound closure and granulation tissue formation *in vivo*. Taken together, these observations strongly suggest that levels of SSW cigarette smoke that can be found in tissues of "second-hand" smokers stimulate cell changes that interfere with processes involving cell migration while simultaneously promoting cell survival.

It is known that cells respond to insults by stimulating the expression/production of survival and stress response proteins. We show that SSW treatment leads to the stimulation of the heat shock protein grp78, the early stress response protein cIL-8, and the survival protein PKB/Akt, suggesting that this level of cigarette smoke exposure results in the immediate stimulation of survival responses against the toxic effects of cigarette smoke. These findings, coupled with the fact that SSW stimulates an increase in the levels of the cell cycle proteins, p53 and p21, suggest that constant stimulation of these proteins may lead not only to a short-term survival response, but also to a more sustained stimulation of cell survival. p53 and p21 have been implicated in cell survival by stimulating processes that allow the cells to repair their DNA [37-39]; p53 binds to the promoter region of p21 and induces the expression of this protein, leading to cell cycle arrest and DNA repair resulting in cell survival.

Our observations that grp78, an ER-specific protein turned on by ER stress, was stimulated by both SSW and nicotine and that nicotine also induced effects similar to those observed with SSW treatment, suggested that nicotine may play a major role in SSW-induced disruption of the endomembrane system. Our work supports that of Peirone [40] who showed that, upon nicotine exposure, the cisternae of the Golgi apparatus were slightly dilated. Although the characteristic pattern remained unchanged, the ends of the apparatus appeared swollen, giving the appearance of vacuoles. In addition, it is known that nicotine readily permeates biological membranes [41]. When nicotine penetrates the plasma membrane, it travels to the ER, the primary site for nicotine metabolism by cytochrome P450 [42-44].

The SSW-induced cellular changes we observed in the cytoskeleton may also have important adverse implications for repair and remodeling. In SSW-treated fibroblasts, the microtubules are not as well organized and the centrosome/MTOC is disrupted. It has been shown that disruption of microtubules causes disorganization of the Golgi and endoplasmic reticulum network and leads to their clustering around the nucleus [45,46]. Therefore, changes in microtubule structural organization may very well affect the distribution of these organelles. In addition, microtubules are major cytoskeletal elements that help carry signaling molecules and organelles to different parts of the cell so that they can perform their functions properly. Therefore, the effects of SSW on microtubule organization may have implications for the effects we observe on the Golgi and endoplasmic reticulum.

SSW also causes an increase in focal adhesion molecules such as vinculin and F-actin that could potentially contribute to the observed decrease in cell migration. These results also suggest a possible mechanism by which individuals exposed to cigarette smoke have impaired healing, because an increase in adhesion may result in a decrease in fibroblast migration into the wound site. During normal wound healing, these cells migrate into the area of damaged tissue, produce growth factors/cytokines, and deposit/remodel the ECM. Therefore, even if fibroblast numbers are sufficient for proper healing, because they are unable to migrate they may remain concentrated at the edge of the wound where they will deposit excess ECM, leading to poor wound closure and abnormal scar formation. These findings have led us to further our studies in a system that more closely mimics the *in vivo* environment. Using mouse model system and special chambers, where the mice smoke, we were able to correlate our *in vitro* findings with *in vivo* results.

Conclusions

Second-hand smoke stimulates proteins that enhance cell survival and inhibit cell migration, processes that may result in abnormal repair and remodeling and/or lead to excess scarring, which are common problems among smoke-exposed individuals. Furthermore, these levels of smoke may interfere with critical functions of detoxification and protein secretion performed by the endomembrane system. These results also may have important implications for diseases such as cancer and fibrosis. Finally, it is our hope that this work will lead eventually to the realization that "second-hand" smoke exposure can be very damaging.

Methods

Reagents

Tissue culture supplies and TRIzol reagent were purchased from Gibco-BRL.

Primary antibodies used

Anti-p21 (Santa Cruz Biotechnology Inc., Santa Cruz, CA), PKB (Cell Signaling Technology Inc., Beverly, MA), p53 (Oncogene Research Products Inc, San Diego, CA.), grp78 (Santa Cruz Biotechnology Inc., Santa Cruz, CA); Anti-β-COP Protein (Sigma Immuno Chemicals, St. Louis, MO); Anti-cIL-8 rabbit serum was produced by Robert Sargeant (Ramona, CA).

Secondary antibodies used

Anti-mouse and anti-rabbit horseradish peroxidase (Amersham: Piscataway, NJ); anti-mouse Alexa (Molecular Probes, Eugene, OR); anti-mouse FITC (Dako Corporation, Carpinteria, CA). The ECL reagents were purchased from Amersham; Vectashield mounting medium from Vector Laboratories (Burlingame, CA); DC protein assay kit from Bio-Rad (Hercules, CA). Nicotine was from Sigma. $DIOC_6$, rhodamine phalloidin, and BODIPY TR ceramide were from Molecular Probes, Inc., (Eugene, OR).

Smoke solution preparation

Sidestream whole (SSW) smoke and mainstream whole (MSW) smoke solutions were made from 2R1 research-grade cigarettes (University of Kentucky, Louisville, KY). MSW and SSW smoke were bubbled into 199 serum free media as previously described by Knoll et al., [10] using a puffer box built by the University of Kentucky. SSW smoke was collected from the burning end of the cigarette and MSW smoke from the opposite end. The pH of the smoke solutions was adjusted to 7.4. The solution is aliquoted and kept frozen (this solution is stable for up to one and a half month at -20°C).

Smoke solution quantification

The smoke solution was quantified according to a previously described protocol. Briefly, 300 μl of each type of smoke solution was used to extract the nicotine after the pH was raised to 10 in order to partition the nicotine into the organic solvent. 1 ml of pentane containing 4 μg/ml of 2-benzylaminopyridine was added as an internal standard. The organic phase was removed and the aqueous phase was extracted again with 1 ml of pure pentane (without internal standard). The extracts were pooled and then evaporated to dryness under a stream of dry nitrogen gas and redissolved in 100 μl of dichloromethane. A 1 μl aliquot was analyzed by gas chromatography using fused-silica DB-1 column (J & W Scientific). Eluted compounds from the column were monitored by flame ionization detection (FID), and the signal was processed by an integrator. Nicotine contents were determined by calculating the ratio between the peak areas for nicotine and the 2-benzylaminopyridine internal standard, and comparing to a standard curve prepared with known amounts of nicotine and internal standard. The correlation coefficient of the standard curve was 0.9995.

Tissue culture

Primary embryonic fibroblasts were prepared from 10-day-old chicken embryos as described previously [47]. Briefly, on day four, primary cultures were trypsinized and plated at a density of 0.3×10^6/35 mm plates in 199 medium (Gibco BRL) containing 0.3% tryptose phosphate broth and 2% donor calf serum, and were allowed to grow for 3 days to become confluent (this density of cells was used for the experiments except where indicated). The fibroblasts were exposed to the smoke solutions at 37°C, 5% CO_2 for varying periods of time.

ATP assay

ATP was measured using the CellTiter-Glo Luminescent Cell Viability Assay kit (Promega, Inc.). The assay was performed according to the manufacturer's protocol with small modifications as briefly detailed below. 3×10^4 cells/well was seeded into a 96 well plate (Costar, Inc.). Fibroblasts were treated with SSW for 18 hours. Half an hour before the end of the treatment, the cells were allowed to equilibrate to room temperature. The substrate was then added and the samples were read in a BMG LUMIstar Galaxy Luminometer.

Flow cytometry

Fibroblasts were plated at 1.2×10^6 cells per 60 mm plate, allowed to grow to confluency and treated for the indicated times. Cells were then trypsinized, centrifuged, and stained with 50 nM DiOC6 (Molecular Probes, Inc.) in warm 1X PBS. They were then rinsed once and resuspended in 1X PBS. Samples were loaded into a FACS machine (Becton Dickinson Immunocytometry Systems) and counted. Excitation was done at 488 nm and emission detected at 530 nm.

BrdU assay

BrdU incorporation assay was performed according to manufacturer's instruction (Oncogene, Inc.). Cells were seeded in a 96 well plate and allowed to grow to confluency. BrdU was added along with the SSW treatment and allowed to incubate for the appropriate time points. The cells were fixed and denatured with manufacturer's Fixative/Denaturing Solution and incubated for 30 minutes at room temperature. The samples were then incubated with anti-BrdU antibody for 1 hour at room temperature and washed 3 times. Peroxidase Goat anti-mouse IgG HRP was added and allowed to incubate for 30 minutes followed by the TMB substrate addition and incubation in the dark for 15 minutes and stopping the reaction and reading the samples at a dual wavelength of 450–570 nm.

Cell growth and survival experiments

Fibroblasts were treated with SSW smoke solution for 18 hours. For the cell growth studies, cells were then trypsinized, resuspended in isoton solution (Coulter Electronics Ltd) and counted in a Coulter counter (Model Z2; Coulter Electronics Ltd.). For survival studies, at the end of the treatment period, fresh media was added and cells were allowed to recover for 24 hours. The next day, the cells were treated again with SSW for 18 hours more. Cells were then typsinized, resuspended in isoton solution (Coulter Electronics Ltd) and counted in a Coulter counter.

Immunoblotting

This procedure was described previously by us [47].

Lysates for PKB/Akt detection

The detection of PKB was done according to manufacturer's protocol (Upstate, Inc.). 2×10^6 cells were seeded in a 35 mm plate until confluency. Cells were incubated in serum-free medium overnight to reduce basal levels of phosphorylation. The following day the cells were incubated with SSW in fresh serum-free medium for the appropriate times. At the end of the treatments cells were washed with 1X PBS, then lysed by adding 1X SDS Sample Buffer containing protease and phosphatase inhibitors, immediately scraped off the plates and transferred to a microcentrifuge tube and kept on ice. The samples were sonicated to shear DNA and reduce sample viscosity, then heated and cooled on ice. After centrifugation, the samples were loaded onto 10% SDS-PAGE gel.

Immunolabeling

Vinculin, β-COP protein, cIL-8, and microtubules were detected by labeling with specific antibodies. Fibroblasts were treated with SSW as described above. The cells were rinsed and fixed in 4% paraformaldehyde, permeabilized with 0.1% Triton X-100 in 1X PBS, and incubated with PBS containing 0.1 M glycine. Cells were blocked with 10% goat or sheep serum in PBS, incubated with mouse anti-β-COP Protein (1:20), anti-cIL-8 (1:200), anti-vinculin (1:50) or anti-tubulin (1:200) in 1% BSA/PBS and washed three times with 0.1% BSA/PBS. The cells were then incubated in goat anti-mouse FITC or sheep anti-mouse Texas Red (1:100) in 1% BSA/PBS, washed 3 times, 10 minutes each, with 0.1% BSA in PBS, and mounted with Vectashield.

Cloning ring migration assay

Fibroblasts were plated in cloning rings (Fisher Scientific, Inc.). Cells were allowed to adhere for 3 hours then treated with the SSW. Migration was measured at 24 hours using a micrometer. We measured the distance from the edge of the cloning ring to where the cells migrated. Six different measurements were made, averages and standard mean error were determined using Sigma Plot.

Transmission electron microscopy

Samples were prepared as described previously [48,49]. Briefly, cells were fixed in 3% gluteraldehyde in a 0.1 M sodium cacodylate buffer, pH 7.4, and postfixed in a 2% aqueous solution of osmium tetroxide at RT. Dehydration was performed using ascending ethanol series and samples were embedded in Spurs epoxy resin. Thin sections were cut and stained with uranyl acetate in 70% ethanol, followed by lead citrate. Microscopy was performed in a CM 300 transmission electron microscope.

DIOC6 and rhodamine phalloidin labeling

Cells were plated as described above, and treated for 4 hours, then washed with 1X PBS and fixed in 4% paraformaldehyde for 20 minutes. At the end of this period, cells were washed in 1X PBS, incubated with 1X PBS containing 0.1% Triton-X-100 for 10 minutes. After another round of washes, cells were incubated with either DIOC6 or Rhodamine Phalloidin at RT for 20 minutes and then washed and mounted in Vectashield. Quantification of filamentous actin: cells were incubated in 0.2% Triton-X-100 for 10 minutes after fixing in 4% paraformaldehyde. 0.1 M NaOH was used to extract the Rhodamine Phalloidin stained F-actin. Fluorescence was measured using a fluorimeter at 550–580 nm.

RT-PCR conditions

Total RNA was extracted using TRIzol reagent from untreated fibroblasts and fibroblasts treated with 1.5 mM nicotine for 1, 3, 6, 12, 18, and 24 hours. RT-PCR was performed using grp78 specific primers and the Promega Access RT-PCR System following the recommended protocol. The reaction conditions included: 5 ng of total RNA, first strand synthesis at 48°C for 45 min, then 95°C for 4 min to inactivate the reverse transcriptase and allow for denaturation of RNA/cDNA/primer. This was followed by second strand synthesis and PCR amplification at 95°C, 60 s; 55°C, 60 s for annealing, 72°C, 90 s for extension at 35 cycles and finally, 72°C for 10 minutes to extend the strands. 3 μl of Quantum mRNA classic 18S primers (Ambion, Inc.) were added to the reaction to produce a control product. Primers used for the amplification of grp78 were: sense primer 5'GAGATCATCGCCAACGATCAG and antisense primer 5'ACTTGATGTCCTGCTGCACAG. 18SrRNA sequence is proprietary information that belongs to Ambion. RT-PCR products were analyzed by electrophoresis in 1.5% agarose.

Densitometry and statistical analysis

Microdensitometry analysis was performed using Scion Image analyzer. All data were expressed as mean ± SEM. Significance was determined using Student's *t* test for

comparison between two means. Means were considered significantly different when $P \leq 0.05$.

List of abbreviations

CEF Chicken Embryonic Fibroblasts

MSW MainStream Whole

SSW SideStream Whole

OD Optical Density

RT-PCR Reverse transcription-polymerase chain reaction

ER Endoplasmic Reticulum

TEM Transmission Electron Microscope

MTOC Microtubule Organizing Center

PKB Protein Kinase B

Grp78 Glucose regulated protein 78

FID Flame Ionization Detection

Authors' contributions

LW carried out all studies except for the EM and ER/Golgi immunolabeling studies. HMG carried out the immunolabeling for the endomembrane studies and JEF carried out the EM studies. MY participated in smoke quantification and EN participated and conceived of the protocol for smoke quantification. MMG conceived and designed the studies with LW, and contributed to manuscript preparation and writing. All authors read and approved the final manuscript.

Acknowledgements

We would like to thank the P. Talbot laboratory for use of the smoking machine, Barbara Walter in L. Owen's laboratory for help with the FACS analysis, F. Sladek for the use of the luminometer. A. Grosovsky for the use of the Coulter counter and X. Liu for the p53 antibody. Many thanks to J. Shyy for the grp78 primer and helpful discussions. We also thank Qi-Jing Li for his help with the confocal pictures, other colleagues in our laboratory for helpful discussions and Melissa Dueck for also reading the final version of the manuscript. Part of this work was performed in the UCR Central Facility for Advanced Microscopy and Microanalysis. This work was partially supported by AHA grant# 0050732Y and TRDRP grant# 10IT-0170.

References

1. Pirkle JL, Flegal KM, Bernert JT, Brody DJ, Etzel RA, Maurer KR: **Exposure of the US population to environmental tobacco smoke: the Third National Health and Nutrition Examination Survey, 1988 to 1991.** *Jama* 1996, **275:**1233-1240.
2. EPA: **Respiratory Health Effects of Passive Smoking: Lung Cancer and Other Disorders.** 1992, **Report Number EPA/600/6-90/006F:**3.1-3.1.
3. Lofroth G: **Environmental tobacco smoke: overview of chemical composition and genotoxic components.** *Mutat Res* 1989, **222:**73-80.
4. Frick WG, Seals R. R., Jr.: **Smoking and wound healing: a review.** *Tex Dent J* 1994, **111:**21-23.
5. Silverstein P: **Smoking and wound healing.** *Am J Med* 1992, **93:**22S-24S.
6. Torok J, Gvozdjakova A, Kucharska J, Balazovjech I, Kysela S, Simko F, Gvozdjak J: **Passive smoking impairs endothelium-dependent relaxation of isolated rabbit arteries.** *Physiol Res* 2000, **49:**135-141.
7. Ueng SW, Lee MY, Li AF, Lin SS, Tai CL, Shih CH: **Effect of intermittent cigarette smoke inhalation on tibial lengthening: experimental study on rabbits.** *J Trauma* 1997, **42:**231-238.
8. Clark RF: **The Molecular and Cellular Biology of Wound Repair.** New York, Plenum Press; 1996.
9. Brown LF, Dubin D, Lavigne L, Logan B, Dvorak HF, Van de Water L: **Macrophages and fibroblasts express embryonic fibronectins during cutaneous wound healing.** *Am J Pathol* 1993, **142:**793-801.
10. Knoll M, Talbot P: **Cigarette smoke inhibits oocyte cumulus complex pick-up by the oviduct in vitro independent of ciliary beat frequency.** *Reprod Toxicol* 1998, **12:**57-68.
11. Al-Delaimy WK, Mahoney GN, Speizer FE, Willett WC: **Toenail nicotine levels as a biomarker of tobacco smoke exposure.** *Cancer Epidemiol Biomarkers Prev* 2002, **11:**1400-1404.
12. Russell MA, Feyerabend C: **Blood and Urinary nicotine in non-smokers.** *Lancet* 1975, **1:**179-181.
13. Schwartz SL, Gastonguay MR, Robinson DE, Balter NJ: **Physiologically based pharmacokinetic modeling of nicotine.** *Nicotine and Related Alkaloids Volume 12*. 1stth edition. London, New York, Chapman & Hall; 1993:255-274.
14. Kyerematen GA, Vesell ES: **Metabolism of nicotine.** *Drug Metab Rev* 1991, **23:**3-41.
15. Song MS, Park YK, Lee JH, Park K: **Induction of glucose-regulated protein 78 by chronic hypoxia in human gastric tumor cells through a protein kinase C-epsilon/ERK/AP-1 signaling cascade.** *Cancer Res* 2001, **61:**8322-8330.
16. Koong AC, Chen EY, Lee AS, Brown JM, Giaccia AJ: **Increased cytotoxicity of chronic hypoxic cells by molecular inhibition of GRP78 induction.** *Int J Radiat Oncol Biol Phys* 1994, **28:**661-666.
17. Mote PL, Tillman JB, Spindler SR: **Glucose regulation of GRP78 gene expression.** *Mech Ageing Dev* 1998, **104:**149-158.
18. Lee M, Choi I, Park K: **Activation of stress signaling molecules in bat brain during arousal from hibernation.** *J Neurochem* 2002, **82:**867-873.
19. Rao RV, Peel A, Logvinova A, del Rio G, Hermel E, Yokota T, Goldsmith PC, Ellerby LM, Ellerby HM, Bredesen DE: **Coupling endoplasmic reticulum stress to the cell death program: role of the ER chaperone GRP78.** *FEBS Lett* 2002, **514:**122-128.
20. Yang GH, Li S, Pestka JJ: **Down-regulation of the endoplasmic reticulum chaperone GRP78/BiP by vomitoxin (Deoxynivalenol).** *Toxicol Appl Pharmacol* 2000, **162:**207-217.
21. Little E, Ramakrishnan M, Roy B, Gazit G, Lee AS: **The glucose-regulated proteins (GRP78 and GRP94): functions, gene regulation, and applications.** *Crit Rev Eukaryot Gene Expr* 1994, **4:**1-18.
22. Yamane A, Shinmura K, Sunaga N, Saitoh T, Yamaguchi S, Shinmura Y, Yoshimura K, Murakami H, Nojima Y, Kohno T, Yokota J: **Suppressive activities of OGG1 and MYH proteins against G:C to T:A mutations caused by 8-hydroxyguanine but not by benzo[a]pyrene diol epoxide in human cells in vivo.** *Carcinogenesis* 2003, **24:**1031-1037.
23. Izzotti A, Bagnasco M, D'Agostini F, Cartiglia C, Lubet RA, Kelloff GJ, De Flora S: **Formation and persistence of nucleotide alterations in rats exposed whole-body to environmental cigarette smoke.** *Carcinogenesis* 1999, **20:**1499-1505.
24. Lee CK, Brown BG, Reed EA, Coggins CR, Doolittle DJ, Hayes AW: **Ninety-day inhalation study in rats, using aged and diluted sidestream smoke from a reference cigarette: DNA adducts and alveolar macrophage cytogenetics.** *Fundam Appl Toxicol* 1993, **20:**393-401.
25. Holz O, Meissner R, Einhaus M, Koops F, Warncke K, Scherer G, Adlkofer F, Baumgartner E, Rudiger HW: **Detection of DNA single-strand breaks in lymphocytes of smokers.** *Int Arch Occup Environ Health* 1993, **65:**83-88.
26. Lee CK, Brown BG, Reed BA, Rahn CA, Coggins CR, Doolittle DJ, Hayes AW: **Fourteen-day inhalation study in rats, using aged**

and diluted sidestream smoke from a reference cigarette. II. DNA adducts and alveolar macrophage cytogenetics. *Fundam Appl Toxicol* 1992, **19:**141-146.
27. Reddy MV, Randerath K: **A comparison of DNA adduct formation in white blood cells and internal organs of mice exposed to benzo[a]pyrene, dibenzo[c,g]carbazole, safrole and cigarette smoke condensate.** *Mutat Res* 1990, **241:**37-48.
28. Nakayama T, Kaneko M, Kodama M, Nagata C: **Cigarette smoke induces DNA single-strand breaks in human cells.** *Nature* 1985, **314:**462-464.
29. Hopkins JM, Evans HJ: **Cigarette smoke-induced DNA damage and lung cancer risks.** *Nature* 1980, **283:**388-390.
30. Piperi C, Pouli AE, Katerelos NA, Hatzinikolaou DG, Stavridou A, Psallidopoulos MC: **Study of the mechanisms of cigarette smoke gas phase cytotoxicity.** *Anticancer Res* 2003, **23:**2185-2190.
31. Wickenden JA, Clarke MC, Rossi AG, Rahman I, Faux SP, Donaldson K, MacNee W: **Cigarette smoke prevents apoptosis through inhibition of caspase activation and induces necrosis.** *Am J Respir Cell Mol Biol* 2003, **29:**562-570.
32. Rajpurkar A, Jiang Y, Dhabuwala CB, Dunbar JC, Li H: **Cigarette smoking induces apoptosis in rat testis.** *J Environ Pathol Toxicol Oncol* 2002, **21:**243-248.
33. Tithof PK, Elgayyar M, Cho Y, Guan W, Fisher AB, Peters-Golden M: **Polycyclic aromatic hydrocarbons present in cigarette smoke cause endothelial cell apoptosis by a phospholipase A2-dependent mechanism.** *Faseb J* 2002, **16:**1463-1464.
34. Aoshiba K, Tamaoki J, Nagai A: **Acute cigarette smoke exposure induces apoptosis of alveolar macrophages.** *Am J Physiol Lung Cell Mol Physiol* 2001, **281:**L1392-401.
35. Hoshino Y, Mio T, Nagai S, Miki H, Ito I, Izumi T: **Cytotoxic effects of cigarette smoke extract on an alveolar type II cell-derived cell line.** *Am J Physiol Lung Cell Mol Physiol* 2001, **281:**L509-16.
36. Ishii T, Matsuse T, Igarashi H, Masuda M, Teramoto S, Ouchi Y: **Tobacco smoke reduces viability in human lung fibroblasts: protective effect of glutathione S-transferase P1.** *Am J Physiol Lung Cell Mol Physiol* 2001, **280:**L1189-95.
37. Helt CE, Rancourt RC, Staversky RJ, O'Reilly MA: **p53-dependent induction of p21(Cip1/WAF1/Sdi1) protects against oxygen-induced toxicity.** *Toxicol Sci* 2001, **63:**214-222.
38. Li Y, Dowbenko D, Lasky LA: **AKT/PKB phosphorylation of p21Cip/WAF1 enhances protein stability of p21Cip/WAF1 and promotes cell survival.** *J Biol Chem* 2002, **277:**11352-11361.
39. Whyte DA, Broton CE, Shillitoe EJ: **The unexplained survival of cells in oral cancer: what is the role of p53?** *J Oral Pathol Med* 2002, **31:**125-133.
40. Peirone S: **Action of Nicotine on Chick Embryo Heart Cells Cultivated in vitro.** *J Submicrosc Cytol* 1974, **6:**339-352.
41. Russell MA, Feyerabend C: **Cigarette smoking: a dependence on high-nicotine boli.** *Drug Metab Rev* 1978, **8:**29-57.
42. Gabriel A, Vessel K, Vessel ES: **Metabolism of Nicotine.** *Drug Metab Rev* 1991, **23:**3-41.
43. Yamazaki H, Inoue K, Hashimoto M, Shimada T: **Roles of CYP2A6 and CYP2B6 in nicotine C-oxidation by human liver microsomes.** *Arch Toxicol* 1999, **73:**65-70.
44. Nakayama H, Okuda H, Nakashima T, Imaoka S, Funae Y: **Nicotine metabolism by rat hepatic cytochrome P450s.** *Biochem Pharmacol* 1993, **45:**2554-2556.
45. Alvarez C, Sztul ES: **Brefeldin A (BFA) disrupts the organization of the microtubule and the actin cytoskeletons.** *Eur J Cell Biol* 1999, **78:**1-14.
46. Valderrama F, Babia T, Ayala I, Kok JW, Renau-Piqueras J, Egea G: **Actin microfilaments are essential for the cytological positioning and morphology of the Golgi complex.** *Eur J Cell Biol* 1998, **76:**9-17.
47. Vaingankar SM, Martins-Green M: **Thrombin aivation of the 9E3/CEF4 chemokine involves tyrosine kinases including c-src and the epidermal growth factor receptor.** *J Biol Chem* 1998, **273:**5226-5234.
48. Martins-Green M: **Origin of the dorsal surface of the neural tube by progressive delamination of epidermal ectoderm and neuroepithelium: implications for neurulation and neural tube defects.** *Development* 1988, **103:**687-706.
49. Martins-Green M, Erickson CA: **Basal lamina is not a barrier to neural crest cell emigration: documentation by TEM and by immunofluorescent and immunogold labelling.** *Development* 1987, **101:**517-533.